Original article

УДК 539.27:669.14.018.294.2

DOI: 10.57070/2304-4497-2023-3(45)-58-71

STRENGTHENING MECHANISMS OF RAIL STEEL UNDER COMPRESSION

© 2023 Yu. F. Ivanov[1], M. A. Porfir'ev[2], V. E. Gromov[2], N. A. Popova[3], Yu. S. Serenkov[2], A. N. Siddiquee[4], V. V. Shlyarov[2]

[1]**Institute of High Current Electronics SB RAS** (2/3 Akademicheskii Ave., Tomsk 634055, Russian Federation)

[2]**Siberian State Industrial University** (42 Kirova Str., Novokuznetsk, Kemerovo Region – Kuzbass, 654007, Russian Federation)

[3]**Tomsk State University of Architecture and Civil Engineering** (Solyanaya Square 2, Tomsk 634003, Russian Federation)

[4]**Jamia Millia Islamia** (Jamia Nagar, New Delhi-110025, India)

Abstract. Strain hardening of steels is an effective approach to changing the structural-phase state and properties. Understanding the mechanisms of formation of structural-phase states and properties of pearlitic steel during plastic deformation is crucial for controlling the process of de-formation behavior. The importance of knowledge in this area is due to serious problems in the field of physical materials science, as well as the practical consequences of the use of pearlitic steel, which is widely used in the railway industry. Currently, there is great interest in understanding the general relationships characterizing strain hardening. This interest is associated with the possibility of developing a complex theory of this phenomenon and studying the dislocation mechanisms that determine the observed stress-strain curves σ(ε). It is noteworthy that advances have been made in the field of strength physics, in particular in understanding the dislocation structure of bainitic and martensitic steels. These advances have contributed to expanding our understanding of strain hardening phenomena. Present work the evolution of structural-phase states and dislocation substructure of rail steel under uniaxial com-pression to the degree of 50 % was studied by transmission electron microscopy. The obtained data formed the basis for a quantitative analysis of the mechanisms of rail steel strengthening at degrees of deformation by compression 15, 30, 50 %. Contributions to the strengthening caused by the friction of matrix lattice, dislocation substructure, presence of carbide particles, internal stress fields, solid solution and substructural strengthening, pearlite component of the steel structure are estimated. Using the adaptivity principle, which as-sumes the independent action of each of the strengthening mechanisms, the dependence of rail steel strength on the degree of plastic deformation by compression is estimated. A com-parative analysis of the stress-strain curves σ(ε) obtained experimentally and calculated theo-retically is performed.

Keywords: stress-strain curve; rail steel; structure; dislocation substructure; strengthening mechanisms; additive yield strength; electron microscopy

For citation: Ivanov Yu.F., Porfir'ev M.A., Gromov V.E., Popova N.A, Serenkov Yu.S, Siddiquee A.N., Shlyarov V.V. Strengthening mechanisms of rail steel under compression. *Bulletin of the Siberian State Industrial University*. 2023, no. 3 (45), pp. 58 – 71. (In Russ.). *http://doi.org/10.57070/2304-4497-2023-3(45)-58-71*

Оригинальная статья

МЕХАНИЗМЫ УПРОЧНЕНИЯ РЕЛЬСОВОЙ СТАЛИ ПРИ СЖАТИИ

© 2023 г. Ю. Ф. Иванов[1], М. А. Порфирьев[2], В. Е. Громов[2], Н. А. Попова[3], Ю. С. Серенков[2], А. Н. Сиддики[4], В. В. Шляров[2]

[1]**Институт сильноточной электроники СО РАН** (Россия, 634055, Томск, пр. Академический, 2/3)

[2]**Сибирский государственный индустриальный университет** (Россия, 654007, Кемеровская обл. – Кузбасс, Новокузнецк, ул. Кирова, 42)

[3]**Томский государственный архитектурно-строительный университет** (Россия, 634003, Томск, пл. Соляная, 2)

[4]**Джамия Миллия Исламия** (Джамиа Нагар, Нью-Дели-110025, Индия)

Аннотация. Деформационное упрочнение сталей – эффективный подход к изменению структурно-фазового состояния и свойств. Понимание механизмов образования структурно-фазовых состояний и свойств перлитной стали при пластической деформации имеет решающее значение для управления процессом деформационного поведения. Важность знаний в этой области обусловлена серьезными проблемами в области физического материаловедения, а также практическими последствиями применения перлитной стали, широко используемой в железнодорожной отрасли. В настоящее время существует большой интерес к пониманию общих зависимостей, характеризующих деформационное упрочнение. Этот интерес связан с возможностью разработки комплексной теории этого явления и исследования дислокационных механизмов, обусловливающих наблюдаемые кривые напряжение – деформация. Примечательно, что были достигнуты успехи в области физики прочности, в частности, в понимании дислокационной структуры бейнитных и мартенситных сталей. Эти достижения способствовали расширению понимания явлений деформационного упрочнения. В настоящей работе методом просвечивающей электронной микроскопии изучена эволюция структурно-фазовых состояний и дислокационной субструктуры рельсовой стали при одноосном сжатии до степени 50 %. Полученные данные легли в основу количественного анализа механизмов упрочнения рельсовой стали при степенях деформации сжатием 15, 30 и 50 %. Проведена оценка вклада в упрочнение, обусловленного трением решетки матрицы, дислокационной субструктурой, наличием карбидных частиц, полями внутренних напряжений, твердорастворным и субструктурным упрочнением, перлитной составляющей структуры стали. С использованием принципа адаптивности, предполагающего независимое действие каждого из механизмов упрочнения, оценена зависимость прочности рельсовой стали от степени пластической деформации сжатием. Проведен сравнительный анализ кривых напряжение – деформация σ(ε), полученных экспериментально и рассчитанных теоретически.

Ключевые слова: кривая напряжение – деформация, рельсовая сталь, состав, дислокационная субструктура, механизмы укрепления, аддитивный предел текучести, электронная микроскопия

Для цитирования: Иванов Ю.Ф., Порфирьев М.А., Громов В.Е., Попова Н.А., Серенков Ю.С., Сиддики А.Н., Шляров В.В. Механизмы упрочнения рельсовой стали при сжатии // Вестник Сибирского государственного индустриального университета. 2023. № 3 (45). С. 58 – 71. *http://doi.org/10.57070/2304-4497-2023-3(45)-58-71*

Introduction

Deformation strengthening of steels is one of the ways to change the structural-phase state and properties characterizing the fracture resistance [1 – 7]. Knowledge of the formation patterns of structural-phase states and properties of pearlite steel during plastic deformation is necessary to control the process of deformation behaviour. The importance of information in this field is determined by the depth of fundamental problems in physical materials science, on the one hand, and the practical significance of the problem, on the other hand, since the rails are made of pearlitic steel [8 – 19].

At present, the general dependencies that characterise strain hardening attract the most interest as they can be applied for constructing a theory of this phenomenon, on the one hand, and studying dislocation mechanisms explaining the observed type of curves σ(ε), on the other. Certain success in development of ideas about dislocation structures of bainitic and martensitic steels has been achieved in strength physics [20]. However, we should note that dislocation steel structure and its evolution during deformation are insufficiently studied. This is especially true of the quantitative parameters of dislocation ensemble. Little attention is paid to fragmentation processes. Internal stress fields were examined mainly by the *X*-ray diffraction method, local stress fields are understudied [21, 22].

The transmission diffraction electron microscopy method, due to its high resolution, makes it possible to conduct in-depth analysis of defects in steels and therefore is the most effective means of detailed investigation of dislocation substructure [23, 24]. Development

Table 1

Chemical composition of the rail steel
Химический состав рельсовой стали

Element	C	Mn	Si	Cr	P	S	Ni	Cu	Ti	Mo	V	Al
Quantity, % (wt.)	0.73	0.75	0.58	0.42	0.012	0.007	0.07	0.13	0.003	0.006	0.04	0.003

of new special types of rails (for high-speed movement, low-temperature reliability, resistance to contact fatigue and wear, etc.) should be based on knowledge of the mechanisms of structural and phase changes and fine substructure under deformation. The mechanisms of rails strengthening at different volumes of the passed tonnage were evaluated in [25 – 28], and the evolution of lamellar pearlite of rail steel under compression deformation was analysed in [29, 30].

The purpose of this work is a comparative analysis of experimental stress-strain curves σ(ε) and the mechanisms of rail steel strengthening, obtained on the basis of a quantitative assessment, under compression deformation.

Research methods and principles

Differentially heat-strengthened rails of DT350 category manufactured by Evraz ZSMK JSC, produced from evacuated electric steel E76KhF in accordance with the technical requirements TU 0921-276-01124333-2021, were studied. The chemical composition of the rail steel is shown in Table 1. Five rectangular samples with a size of 5×5×10 mm were cut from the rail head and subjected to deformation. Uniaxial compression deformation was carried out at a room temperature on Instron 3369 (Great Britain) testing machine at a loading speed of 1.2 mm/min.

The steel structure was studied using transmission electron diffraction microscopy (JEOL JEM 2100F, Japan). The objects of research for transmission electron microscopy (foils ranging in thickness from 150 to 200 nm) were made by electrolytic thinning of plates cut by methods of electric spark erosion of metal from the central part of the sample in the direction perpendicular to the compression axis. The structural and phase state of steel subjected to deformation by 15, 30 and 50 % was analysed.

The images of the material fine structure obtained during its examination in the electron microscope were necessary to identify the morphological components of the structure and their volume fractions, determine the size, distribution density and volume fraction of cementite particles, as well as their localization, and define the parameters of the material fine structure in each morphological component (scalar ρ and excess $\rho_{\pm}$ dislocation density, amplitudes of curvature-torsion of the crystal lattice χ and internal stresses).

The volume fractions of morphological components were determined by the planimetric method measuring the total cross-sectional area of the given structural component on a certain area of the foil [31]:

$$\delta = \frac{1}{St}\sum_{i=1}^{n} S_{ni}, \qquad (1)$$

where S_t – total area of the image; $\sum_{i=1}^{n} S_{n_i}$ – total surface area, occupied by the corresponding morphological component of the structure. The volume fractions were defined by the continuous sections of the sample with an area of ~100 μm^2 at a magnification in the microscope column of ~10000 times.

The sizes of cementite particles and the distances between them were determined in each morphological component by micrographs using direct measurement [32]. In pearlite of lamellar morphology (not destroyed pearlite), only the transverse size of cementite particles was measured, in a ferrite-carbide mixture (destroyed pearlite) and fragmented perlite – the longitudinal and transverse dimensions, in steel deformed to ε = 50 % – only diameter:

$$\overline{R} = \frac{1}{N}\cdot\sum_{i=1}^{N} N_i R_i; \quad \overline{L} = \frac{1}{N}\cdot\sum_{i=1}^{N} N_i L_i, \qquad (2)$$

where N_i – number of particles in a given size class; R_i and L_i – average transverse and longitudinal particle sizes, in this class; n – number of classes; N – total number of measurements.

The number of measurements ranged from 40 to 50.

The average distance between cementite particles was determined by the secant method using microphotographs [32].

The volume fraction of particles of carbide phases in the body of structural components was determined by the formula [33]:

$$\delta = V_p / tr^2, \qquad (3)$$

where V_p – average particle volume; t – foil thickness; r – distance between particles.

The scalar density of dislocations in each morphological component of the steel structure was determined by the methods [23]. Its values were calculated using the formula:

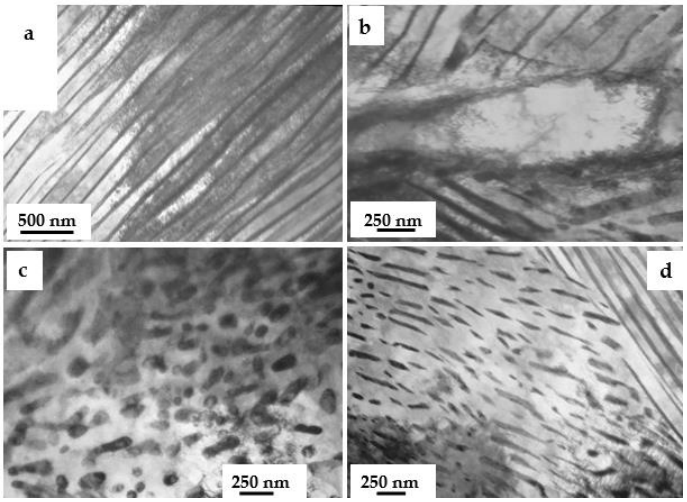

Fig. 1. TEM images of the rail structure before deformation
Рис. 1. Изображения рельсовой конструкции до деформации

$$<\rho>=\frac{M}{t}\left(\frac{n_1}{l_1}+\frac{n_2}{l_2}\right), \quad (4)$$

where n_1 and n_2 – number of intersections of horizontal and vertical lines with length l_1 and l_2 by dislocations; M – magnification of the micrograph; t – foil thickness (200 nm).

The average scalar dislocation density was determined taking into account the volume fraction of each type of morphological components of the steel structure according to the formula:

$$<\rho>=\sum_{i=1}^{z} P_{vi}\rho_i\,, \quad (5)$$

where P_{Vi} – volume fraction of the material occupied by the i-th type of morphological component of the steel structure; Z – its volume fraction; ρ_i – scalar density of dislocations in this morphological component.

The excess dislocation density was calculated by the disorientation gradient:

$$\rho\pm=\frac{1}{b}\frac{\partial\varphi}{\partial\lambda} \quad (6)$$

where b – Burgers vector; $\chi = \partial\varphi/\partial\lambda$ – amplitude of the curvature-torsion of the crystal lattice; $\partial\varphi$ – inclination angle of the foil in the microscope column; $\partial\lambda$ – displacement of the extinction contour.

Results and Discussion

Transmission electron microscopy of thin foils established that the steel structure is represented by pearlite grains of plate morphology (Fig. 1, *a*), grains of structurally free ferrite (ferrite grains that do not contain carbide particles in the bulk phases) (Fig. 1, *b*) and ferrite grains, in the volume of which cementite particles are observed mainly in the form of short plates (Fig. 1, *d*), and globular particles (Fig. 1, *c*). As a rule, the volumes of steel with globular particles and particles in the form of short plates are observed separately, which made it possible to estimate their relative content in the material being equal to 1:10.

It can be noted that the relative volume fraction of grains of structurally free ferrite is small and varies from 0.01 to 0.05 of the steel structure. The relative volume fraction of grains of the ferrite-carbide mixture is significantly weightier, the value of which varies in the range from 0.17 to 0.27 of the steel structure. Dislocation substructure is observed in the grain volume mainly in the form of chaotically distributed dislocations.

Plastic deformation of steel is accompanied by fragmentation of the ferritic component of steel, which becomes stronger as the degree of deformation increases. *At* ε = 50 %, the fragmented structure of steel occupies 0.4 of the volume of the examined foil. As the degree of deformation rises, the average sizes of ferrite plate fragments decrease from 240 nm (ε = 15 %) to 200 nm (ε = 50 %).

Analysis of the steel structure by transmission electron microscopy of thin foils demonstrated the presence of bend extinction contours in the electron microscopic images of pearlite grains a typical image of which is shown in Fig. 2.

The presence of bend extinction contours indicates curvature-torsion of the crystal lattice of the analysed foil region. The performed studies show that the sources of curvature-torsion of the crystal lattice (stress concentrators) are mainly the interfaces between ferrite and cementite plates. In most of the observed cases, the contours are located perpendicular to the interface (Fig. 2, *a*). The source of the curvature-torsion of the crystal lattice of the material can also be the ends of the cementite plates (Fig. 2, *b*, *c*), as well as the interfaces of pearlite grains (Fig. 2, *d*).

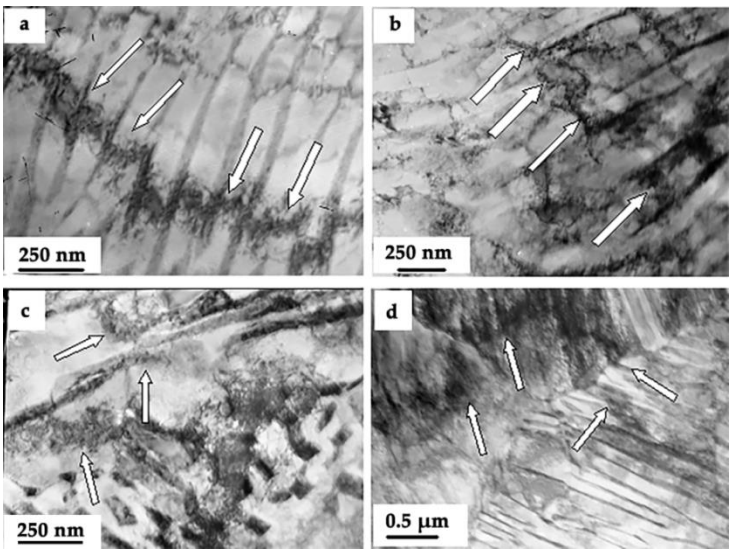

Fig. 2. Electron microscopic image of bend extinction contours (indicated by arrows) (ε = 30 %)
Рис. 2. Электронно-микроскопическое изображение контуров экстинкции изгиба (обозначено стрелками) (ε = 30 %)

Dissolution and cutting of cementite plates are observed simultaneously with the fragmentation of ferrite plates. Carbon atoms, transferred from the cementite crystal lattice to dislocations, are carried into the interplate space and form nanoscale (15 – 20 nm) cementite particles.

In the research literature, two mechanisms of destruction of cementite plates during the deformation of steel with a pearlite structure are mainly discussed. The first of them consists in cutting the plates by moving dislocations and carrying carbon atoms into ferrite in the field of dislocation stresses (Fig. 3, *a*). The estimates show, that in this case, the maximum effect of cementite decomposition cannot exceed tenths of a percent of the available amount of cementite.

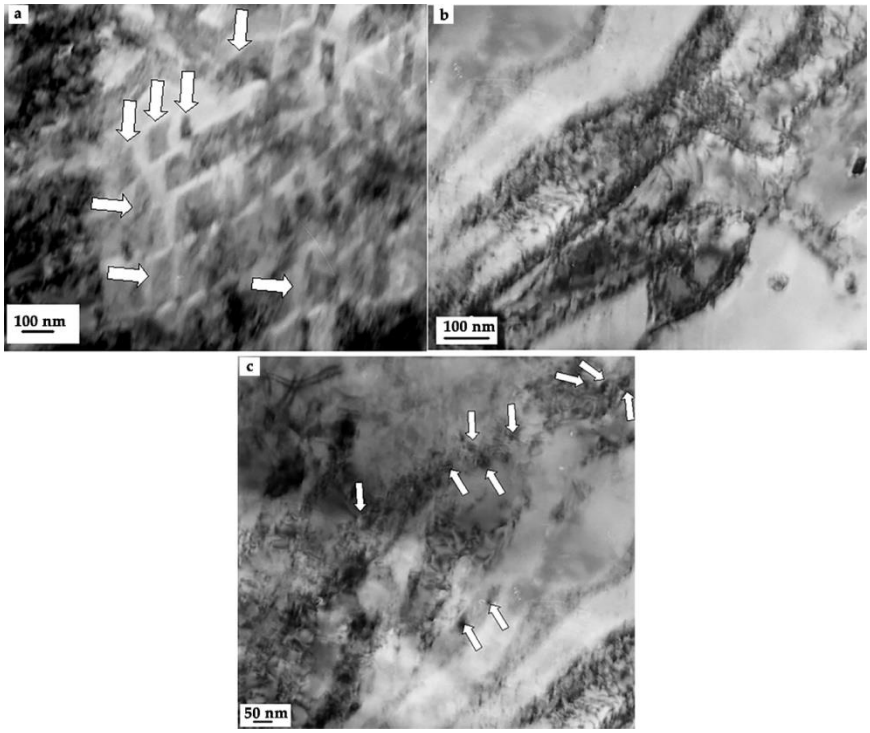

Fig. 3. TEM image of the structure of a pearlite colony at the stage of cutting cementite plates (indicated by arrows) by gliding dislocations (ε = 15 %) (*a*); at the stage of dissolution (ε = 30 %) (*b*); at the stage of the formation of nanosized cementite particles (indicated by arrows) (ε = 50 %) (*c*)
Рис. 3. ПЭМ-изображение структуры колонии перлита на стадии разрезания пластин цементита (обозначено стрелками) скользящими дислокациями (ε = 15 %) (*a*); на стадии растворения (ε = 30 %) (*b*); на стадии формирования наноразмерные частиц цементита (обозначены стрелками) (ε = 50 %) (*c*)

The second mechanism consists in the pulling of carbon atoms from the lattice of the carbide phase during the plastic deformation by dislocations (Fig. 3, *b*). Because of a noticeable difference in the average binding energy of carbon atoms with dislocations (0.6 eV) and with iron atoms in the cementite lattice (0.4 eV) this process leads to the formation of Cottrell atmospheres [29]. At the next stage of cementite dissolution, the entire volume of the material previously occupied by the cementite plate is filled with nanosized particles. A typical image of the resulting structure is shown in Fig. 3, *c*.

The steel deformation is accompanied by transformation of dislocation substructure, namely, the quasi-homogeneous distribution of dislocations of the original steel is replaced by clusters of dislocations around cementite particles.

Samples of E76KhF steel could not be brought to fracture during compression test. They were flattened because the steel under study is capable of deforming quite strongly without fracturing. In [29, 30] we showed that the deformation strengthening of the examined steel during plastic deformation by uniaxial compression has a multi-stage character.

The revealed transformations of the steel structure will significantly affect the strength and plastic characteristics of the metal, determining the service life of the product. Evaluation of strengthening mechanisms allows the patterns connecting the parameters of the structure and the strength properties of the material to be identified and the physical nature of the evolution process of properties to be revealed. The evaluation of the hardening mechanisms was carried out using the widely tested expressions given below.

The main contributions to the deformation resistance are [33, 34]: σ_0 = 35 MPa – the friction stress of dislocations in the crystal lattice of α-iron; σ_{ss} – strengthening of a ferrite-based solid solution by atoms of alloying elements; σ_p – strengthening due to pearlite; σ_h – strengthening by dislocations "herringbone" that cut the slipping dislocations; σ_{or} – strengthening of the material by incoherent particles when bypassing them with dislocations according to Orowan mechanism; σ_l – strengthening by the internal long-range stress fields; σ_s – substructural strengthening.

The evaluation of the solid-solution strengthening of steel caused by carbon atoms and other alloying elements was performed using the empirical expression of the form [33]:

$$\sigma_{ss} = \sum_{i=1}^{n} C_i k_i, \qquad (7)$$

where k_i – strengthening coefficient of ferrite, which is an increase in the strength of the material at the yield point with 1 wt. % of the alloying element is dissolved in it, the value of which for various elements is determined empirically; C_i – concentration of the *i*-th element dissolved in ferrite, wt. %.

By the *i*-th element, we mean elements in quantities available at that moment in the α-solid solution.

Hardening caused by pearlite is determined by the ratio [33]:

$$\sigma_\rho = k_h (4.75r)^{-1/2} Pv, \qquad (8)$$

where P_V – volume fraction of pearlite; r – distance between Fe_3C particles; k_h = $2\cdot10^{-2}$ Pa·m$^{1/2}$ – strengthening coefficient of ferrite.

The stress required to maintain plastic deformation, i.e. the stress of the flow σ required to overcome the forces of interaction with stationary dislocations (dislocations of the "herringbone") by moving dislocations (carriers of deformation), is related to the scalar density of dislocations by the following relation:

$$\sigma_h = m\alpha Gb\sqrt{\rho}, \qquad (9)$$

where m – orientation multiplier (or Schmid factor); α – dimensionless coefficient varying within 0.05 – 0.60 depending on the type of dislocation ensemble (in this work α = 0.25, $m\alpha$ = 1); G – hear modulus of the matrix material (G = 80 GPa); b – Burgers vector of the dislocation (0.25 nm); ρ – the average value of the scalar dislocation density.

Steel strengthening, taking into account the presence of incoherent particles of the second phase, was carried out using the ratio [34]:

$$\sigma_{or} = B\frac{mGb}{2\pi(|r-R|)}\phi\ln\left(\left|\frac{r-R}{2b}\right|\right), \qquad (10)$$

where R – average particle size; r – distance between particle centers; Φ – multiplier depending on the type of dislocation (Φ = 1); B – parameter that takes into account the uneven distribution of particles in the matrix (B = 0.85).

Deformation is accompanied by the formation of internal stress fields in the steel. The magnitude of the plastic component of the internal stress fields can be estimated based on the ratio:

$$\sigma_{\rho l} = m\alpha Gb\sqrt{p_\pm}\,. \qquad (11)$$

The value of the elastic component of the internal stress fields is estimated based on the ratio:

T a b le 2

Quantitative parameters of steel structure in various morphological components with different degrees of plastic deformation

Количественные параметры структуры стали в различных морфологических компонентах при различной степени пластической деформации

Structure parameters		Pearlite			Ferrite	
		Non-fractured	Fractured	Fragmented	Non-fragmented	Fragmented
ε = 15 %						
Vol. fraction		70 %	24 %	3 %	1 %	2 %
Transverse size of the α-phase interlayer, nm		160	120	120		
Fragment size, nm		–	–	120×400	–	400
Fe_3C	size, nm	d = 16	12×280	12×160		
	vol. fraction	12 %	8.7 %	1.5 %		
Fraction of carbon		0.8 %	0.6 %	0.11 %		
$\rho_\alpha \times 10^{-10}$, cm^{-2}		1.91	2.06	2.08	2.21	~0
$\rho_\pm \times 10^{-10}$, cm^{-2}		1.54	1.96	2.08	2.21	
$\chi = \chi_{pl} + \chi_{el}$, cm^{-1}		385	490	$650 = 520_{pl} + 30_{el}$	$1090 = 550_{pl} + 140_{el}$	$745 = 0_{pl} + 745_{el}$
ε = 30 %						
Vol. fraction		65 %	20 %	12 %	0	3 %
Transverse size of the α-phase interlayer, nm		160	120	120		
Fragment size, nm		–	–	120×200	–	200
Fe_3C	size, nm	d = 18	16×280	12×160		
	vol. fraction	12 %	4.8 %	0.92 %		
Fraction of carbon		0.8 %	0.34 %	0.07 %		
$\rho_\alpha \times 10^{-10}$, cm^{-2}		2.18	2.50	1.59		~0
$\rho_\pm \times 10^{-10}$, cm^{-2}		1.76	2.26	1.59		
$\chi = \chi_{pl} + \chi_{el}$, cm^{-1}		440	565	$435 = 395_{pl} + 40_{el}$		$745 = 0_{pl} + 745_{el}$
ε = 50 %						
Vol. fraction		0	60 %	40 %	0	0
Fragment size, nm				200		
Fe_3C in the α-phase (inside fr.)	size, nm		d = 12; r = 16	d = 16; r = 20		
	vol. fraction		1.8 %	2.7 %		
Fraction of carbon in α-phase			0.12 %	0.19 %		
Fe_3C in the layers of Fe_3C (on border of fr.)	size, nm		d = 14; r = 20	d = 16; r = 30		
	Vol. fraction		2.7 %	1.2 %		
Fraction of carbon			0.19 %	0.09 %		
$\rho_\alpha \times 10^{-10}$, cm^{-2}			2.25	0		
$\rho_\pm \times 10^{-10}$, cm^{-2}			2.25			
$\chi = \chi_{pl} + \chi_{el}$, cm^{-1}			$575 = 560_{pl} + 15_{el}$	$55 = 0_{pl} + 55_{el}$		

Table 3

Average material parameters of the steel fine structure at different degrees of plastic deformation
Средние параметры материала тонкой структуры стали
при различных степенях пластической деформации

Average structure parameters	ε = 15 %	ε = 30 %	ε = 50 %
$\rho_{\alpha}\times10^{-10}$, cm^{-2}	1.92	2.11	1.35
$\rho_{\pm}\times10^{-10}$, cm^{-2}	1.63	1.79	1.35
$\chi = \chi_{pl} + \chi_{el}$, cm^{-1}	$425 = 410_{pl} + 15_{el}$	$470 = 445_{pl} + 25_{el}$	$365 = 335_{pl} + 30_{el}$

Table 4

Values of the contributions of various mechanisms into steel strengthening in various morphological components and in general for the material at different degrees of plastic deformation
Значения вклада различных механизмов в упрочнение стали в различных морфологических компонентах и в целом для материала при различных степенях пластической деформации

Contributions	Pearlite			Ferrite		In the material
	Non-fractured	Fractured	Fragmented	Non-fragment	Fragmented	
ε = 15 %						
Vol. fraction	70 %	24 %	3 %	1 %	2 %	100 %
σ_h, MPa	275	285	290	295	0	273
σ_{pl}, MPa	250	280	290	295	0	254
σ_{el}, MPa	0	0	40	190	1010	20
σ_s, MPa	–	–	550	–	350	25
σ_0, MPa	35	35	35	35	35	35
σ_{ss}, MPa	80	80	260	1400	1400	130
σ_p, MPa	570	250	0			460
σ_{or}, MPa			135	0	0	5
ε = 30 %						
Vol. fraction	65 %	20 %	12 %	0	3 %	100 %
σ_h, MPa	295	315	250		0	285
σ_{pl}, MPa	265	300	250		0	262
σ_{el}, MPa	0	0	55		1010	35
σ_s, MPa	–	–	835		750	125
σ_0, MPa	35	35	35		35	35
σ_{ss}, MPa	80	315	190		1400	180
σ_p, MPa	570	250	0			420
σ_{or}, MPa			135			15
ε = 50 %						
Vol. fraction	0	60 %	40 %	0	0	100 %
σ_h, MPa		300	0			180
σ_{pl}, MPa		300	0			180
σ_{el}, MPa		20	75			95
σ_s, MPa		–	750			300
σ_0, MPa		35	35			35
σ_{ss}, MPa		315	300			310
σ_p, MPa		250	0			150
σ_{or}, MPa		1120	645			930

$$\sigma_{el} = m\alpha G t \chi_{el}, \quad (12)$$

where t – thickness of the foil, assumed to be 200 nm; χ_{el} – elastic component of the curvature-torsion of the crystal lattice.

It was noted above that plastic deformation of steel is accompanied by intense material fragmentation. Steel strengthening during the formation of fragments (substructural strengthening) can be estimated based on the ratio [33]:

$$\sigma_s = k_s d^{-1}, \quad (13)$$

where k_s = *150 N/m; d* – size of the formed fragments.

The general steel strengthening in the first approximation, based on the principle of additivity, which assumes the independent action of each of the hardening mechanisms of the material, can be represented as a linear sum of the contributions of individual strengthening mechanisms [33]. However, it was proved that for dislocation mechanisms acting locally and inhomogeneously inside a single grain, such as σh and σl, and which turn out to be different in amplitude, place of action and physical meaning, summation should be performed in a quadratic approximation. Thus, the total strengthening of steel should be calculated according to the formula:

$$\sigma = \sigma_0 + \sigma_{ss} + \sigma_p + \sigma_{or} + \sigma_s + \sqrt{\left(\sigma_l^2 + \sigma_h^2\right)}. \quad (14)$$

The results of the quantitative analysis of the steel structure obtained in this work, as well as in [29, 30], are presented in Tables 2 and 3. This made it possible to evaluate the mechanisms of steel strengthening both in each morphological component and to determine the role of each contribution to the overall steel strengthening (Table 4).

Analysing the results given in Table 4, we can note, firstly, that the strength of steel is a multifactorial value and is determined by the combined action of a number of physical mechanisms. Secondly, the strength of the metal rails depends on the degree of deformation by compression. Thirdly, the strength of the metal increases significantly at large degrees of deformation. The results of summing the contributions of the identified mechanisms to the steel strengthening, performed in the additive approximation, are presented in Fig. 4, *b*. It is clearly seen that the performed estimates are in good qualitative agreement with the behaviour of the experimental stress-strain curve (Fig. 4, *a*). The quantitative discrepancy between the corresponding experimentally obtained and estimated values of steel strength varies within 13 – 28 %. It can be assumed that one of the reasons for this discrepancy is the heterogeneity of the steel structure (the presence of grains of lamellar pearlite and grains of ferrite-carbide mixture), which, having different strengths, will make adjustments to the deformation behaviour of steel.

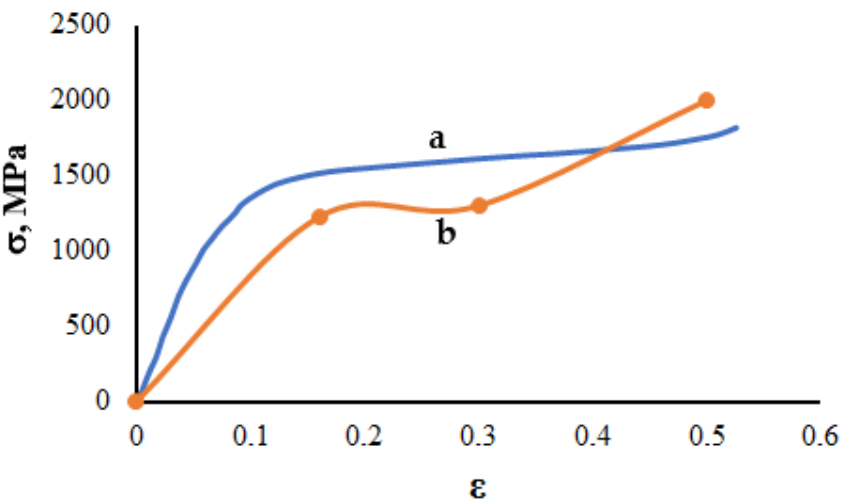

Fig. 4. Dependence σ – ε of rail steel subjected to uniaxial compression loading:
a – experimental curve; *b* – theoretical curve
Рис. 4. Зависимость σ – ε рельсовой стали, подвергнутой одноосному сжатию:
а – экспериментальная кривая; *б* – теоретическая кривая

Conclusions

Evaluation of strengthening mechanisms at various stages of steel deformation was carried out using the quantitative results of the study of steel structure subjected to uniaxial compression deformation. It is shown that the main strengthening factor of the examined steel at the initial stage (≈15 %) is the presence of lamellar pearlite grains. As the deformation degree rises, the role of this factor decreases due to the destruction of cementite plates. An increase in the deformation degree is accompanied by a decrease in the contribution to the steel strengthening from scalar and excessive dislocation density, which is associated with the drifting of dislocations into the boundaries of fragments. The role of contribution of the formation of a solid solution (due to the dissolution of cementite), fragmentation (due to a decrease in the size of fragments and an increase in the relative content of the fragmented structure) and incoherent particles of the carbide phase to the steel strengthening rises with the increase in the degree of steel deformation. A good qualitative agreement of the experimentally obtained and calculated values of steel strength was revealed. The revealed quantitative discrepancy between the corresponding experimentally obtained and estimated values of steel strength might be conditioned by the heterogeneity of steel structure, namely, the presence of grains of lamellar pearlite and grains of ferrite-carbide mixture, which, having different strength, will make adjustments to the deformation behaviour of the material.

СПИСОК ЛИТЕРАТУРЫ

1. Батаев А.А., Батаев И.А., Никулина А.А., Попелюх А.И., Балаганский И.А., Плотникова Н.В. Структурные преобразования углеродистых ферритно-перлитных сталей в условиях высокоскоростного нагружения // Обработка металлов. Технология. Оборудование. Инструменты. 2019. Т. 21. № 3. С. 115–128. *https://doi.org/10.17212/1994-6309-2019-21.3-115-128*
2. Klevtsov G.V., Valiev R.Z., Klevtsova N.A., Zaripov N.G., Karavaeva M.V. Strength and fracture mechanisms of nanostructured metallic materials under single kinds of loading // Metal Science and Heat Treatment. 2018. Vol. 59. No. 9–10. P. 54–62. *https://doi.org/10.1007/s11041-018-0197-2*
3. Yang Cao, Song Ni, Xiaozhou Liao, Min Song, Yuntian Zhu Structural evolutions of metallic materials processed by severe plastic deformation // Materials Science and Engineering: R: Reports. 2018. Vol. 133. P. 1–59. *https://doi.org/10.1016/j.mser.2018.06.001*
4. Gubicza J. Lattice defects and their influence on the mechanical properties of bulk materials processed by severe plastic deformation // Materials Transactions. 2019. Vol. 60. No. 7. P. 1230–1242. *https://doi.org/10.2320/ matertrans.MF201909*
5. Mazilkin A., Straumal B., Kilmametov A., Straumal P., Baretzky B. Phase transformations induced by severe plastic deformation // Materials Transactions. 2019. Vol. 60. No. 8. P. 1489–1499. *https://doi.org/10.2320/ matertrans.MF201938*
6. Blank V.D., Popov M.Yu., Kulnitskiy B.A. The Effect of severe plastic deformations on phase transitions and structure of solids // Materials Transactions. 2019. Vol. 60. No. 8. P. 1500–1505. *https://doi.org/10.2320/ matertrans.MF201942*
7. Bubnov V.A., Korotovskikh V.K., Kostenko S.G. Effect of the degree of plastic deformation on hardness of austenitic steel // Chemical and Petroleum Engineering. 2022. Vol. 57. No. 11012. P. 1038–1042. *https://doi.org/10.1007/s10556-022-01043-x*
8. Wang Y., Tomota Y., Harjo S., Gong W., Ohmuraa T. In-situ neutron diffraction during tension-compression cyclic deformation of a pearlite steel // Materials Science and Engineering: A. 2016. Vol. 676. P. 522–530. *https://doi.org/10.1016/j.msea.2016.08.122*
9. Pan R., Ren R., Chen C., Zhao X. Formation of nanocrystalline structure in pearlitic steels by dry sliding wear // Materials Characterization. 2017. Vol. 132. P. 397–404. *https://doi.org/10.1016/j.matchar.2017.05.031*
10. Steenbergen M. Rolling contact fatigue: Spalling versus transverse fracture of rails // Wear. 2017. Vol. 380-381. P. 96–105. *https://doi.org/10.1016/j.wear.2017.03.003*
11. Vinogradov A., Estrin Y. Analytical and numerical approaches to modelling severe plastic deformation // Progress in Materials Science. 2018. Vol. 95. P. 172–242. *https://doi.org/10.1016/j.pmatsci.2018.02.001*
12. Nikas D., Zhang X., Ahlström J. Evaluation of local strength via microstructural quantification in a pearlitic rail steel deformed by simultaneous compression and torsion // Materials Science and Engineering: A. 2018. Vol. 737. P. 341–347. *https://doi.org/10.1016/j.msea.2018.09.067*
13. Skrypnyk R., Ekh M., Nielsen J.C.O., Pålsson B.A. Prediction of plastic deformation and wear in railway crossings – Comparing the performance of two rail steel grades // Wear. 2019. Vol. 428-429. P. 302–314. *https://doi.org/10.1016/j.wear.2019.03.019*

14. Rong K-j., Xiao Ye-l., Shen M-x., Zhao H-p., Wang W-J., Xiong G-Y. Influence of ambient humidity on the adhesion and damage behavior of wheel–rail interface under hot weather condition // Wear. 2021. Vol. 486-487. Article 204091. *https://doi.org/10.1016/j.wear.2021.204091*

15. Li X.C., Ding H.H., Wang W.J., Guo J., Liu Q.Y., Zhou Z.R. Investigation on the relationship between microstructure and wear characteristic of rail materials // Tribology International. 2021. Vol. 163. Article 107152. *https://doi.org/10.1016/j.triboint.2021.107152*

16. Miranda R.S., Rezende A.B., Fonseca S.T., Sinatora A., Mei P.R. Fatigue and wear behavior of pearlitic and bainitic microstructures with the same chemical composition and hardness using twin-disc tests // Wear. 2022. Vol. 494-495. Article 204253. *https://doi.org/10.1016/j.wear.2022.204253*

17. Pereira H.B., Dias Alves L.H., Rezende A.B., Mei P.R., Goldenstein H. Influence of the microstructure on the rolling contact fatigue of rail steel: Spheroidized pearlite and fully pearlitic microstructure analysis // Wear. 2022. Vol. 498-499. Article 204299. *https://doi.org/10.1016/j.wear.2022.204299*

18. Pan R., Chen Yu., Lan H., Ren R. Investigation into the microstructure evolution and damage on rail at curved tracks // Wear. 2022. Vol. 504-505. Article 204420. *https://doi.org/10.1016/j.wear.2022.204420*

19. Zhang S-Yu., Spiryagin M., Lin Q., Ding H-h., Wu Q., Guo J., Liu Q-Yu., Wang W-J. Study on wear and rolling contact fatigue behaviours of defective rail under different slip ratio and contact stress conditions // Tribology International. 2022. Vol. 169. Article 107491. *https://doi.org/10.1016/j.triboint.2022.107491*

20. Ivanov Yu.F., Gromov V.E., Nikitina E.N. Bainitic constructional steel. Structure and Hardening Mechanisms. Cambridge, 2017. 121 p.

21. Yildirim C., Jessop C., Ahlström J., Detlefs C., Zhang Y. 3D mapping of orientation variation and local residual stress within individual grains of pearlitic steel using synchrotron dark field X-ray microscopy // Scripta Materialia. 2021. Vol. 197. Article 113783. *https://doi.org/10.1016/j.scriptamat.2021.113783*

22. Rybin V.V. Large plastic deformations and destruction of metals. Moscow: Metallurgy, 1986. 224 p.

23. Hirsch P., Hovey A., Nicholson P., Pasley D., Whelan M. Electron microscopy of thin crystals. United Kingdom: Butterworth/Heinemann, 1968. 574 p.

24. Carter C.B., Williams D.B. Transmission Electron Microscopy. Berlin: Springer International Publishing, 2016. 518 p.

25. Ivanov Yu.A., Gromov V.E., Yuriev A.A., Kormyshev V.E., Rubannikova Yu.A., Semin A.P. Deformation strengthening mechanisms of rails in extremely long-term operation // Journal of Materials Research and Technology. 2021. Vol. 11. P. 710–718. *https://doi.org/10.1016/j.jmrt.2020.12.107*

26. Yuriev A.A., Ivanov Yu.F., Gromov V.E., Rubannikova Yu.A., Starostenkov M.D., Tabakov P.Y. Structure and properties of lengthy rails after extreme long-term operation. Millersville: PA, USA: Materials Research Forum LLC, 2021. 194 p. *https://doi.org/10.21741/9781644901472*

27. Иванов Ю.Ф., Юрьев А.А., Чэнь С., Костерев В.В., Громов В.Е. Физическая природа механизмов упрочнения при экстремально длительной эксплуатации рельсов // Известия Алтайского государственного университета. 2021. Т. 117. № 1. С. 33–39. *https://doi.org/10.14258/izvasu(2021)1-05*

28. Ivanov Yu.F., Glezer A.M., Kuznetsov R.V., Gromov V.E., Shliarova Yu.A., Semin A.P., Sundeev R.V. Fine structure formation in rails under ultra long-term operation // Materials Letters. 2022. Vol. 309. No. 4. Article 131378. *http://dx.doi.org/10.1016/j.matlet.2021.131378*

29. Ivanov Yu.F., Gromov V.E., Aksenova K.V., Kuznetsov R.V., Kormyshev V.E., Vashchuk E.S. Evolution of the structure of rail steel during compression // Russian Metallurgy (Metally). 2022. Vol. 10. P. 1192–1197. *https://doi.org/10.1134/S0036029522100354*

30. Аксенова К.В., Громов В.Е., Иванов Ю.Ф., Ващук Е.С., Перегудов О.А. Эволюция структуры пластинчатого перлита рельсовой стали при деформации сжатием // Известия вузов. Черная металлургия. 2022. Т. 65. № 9. С. 654–661. *https://doi.org/10.17073/0368-0797-2022-9-654-661*

31. Салтыков С.А. *Стереометрическая металлография*. Москва: Металлургия. 1970. 376 с.

32. Чернявский К.С. *Стереология в металловедении*. Москва: Металлургия. 1970, 376 с.

33. Гольдштейн М.И., Фарбер В.М. *Дисперсионное упрочнение стали* Москва: Металлургия, 1979. 208 с.

34. Yao M.J., Welsch E., Ponge D., Haghighat S.M.H., Sandlöbes S., Choi P., Herbig M., Bleskov I., Hickel T., Lipinska-Chwalek M., Shantraj P., Scheu C., Zaefferer S., Gault B., Raabe D. Strengthening and strain hardening mechanisms in a precipitation-hardened high-Mn lightweight steel // Acta Materia. 2017.

Vol. 140. P. 258–273. *https://doi.org/ 10.1016/j.actamat.2017.08.049*

REFERENCES

1. Bataev A.A., Bataev I.A., Nikulina A.A., Popelyukh A.I., Balaganskii I.A., Plotnikova N.V. Structural transformations of carbon ferrite-pearlite steels under high-speed loading conditions. *Obrabotka metallov. Tekhnologiya. Oborudovanie. Instrumenty*. 2019, vol. 21, no. 3, pp. 115–128. *https://doi.org/10.17212/1994-6309-2019-21.3-115-128*
2. Klevtsov G.V., Valiev R.Z., Klevtsova N.A., Zaripov N.G., Karavaeva M.V. Strength and fracture mechanisms of nanostructured metallic materials under single kinds of loading. *Metal Science and Heat Treatment*. 2018, vol. 59, no. 9-10, pp. 54–62. *https://doi.org/10.1007/ s11041-018-0197-2*
3. Cao Y., Ni S., Liao X., Song M., Zhu Y. Structural evolutions of metallic materials processed by severe plastic deformation. *Materials Science and Engineering: R: Reports.* 2018, vol. 133, pp. 1–59. *https://doi.org/10.1016/ j.mser.2018.06.001*
4. Gubicza J. Lattice defects and their influence on the mechanical properties of bulk materials processed by severe plastic deformation. *Materials Transactions*. 2019, vol. 60, no. 7, pp. 1230–1242. *https://doi.org/10.2320/ matertrans.MF201909*
5. Mazilkin A., Straumal B., Kilmametov A., Straumal P., Baretzky B. Phase transformations induced by severe plastic deformation. *Materials Transactions.* 2019, vol. 60, no. 8, pp. 1489–1499. *https://doi.org/10.2320/ matertrans.MF201938*
6. Blank V.D., Popov M.Yu., Kulnitskiy B.A. The Effect of severe plastic deformations on phase transitions and structure of solids. *Materials Transactions*. 2019, vol. 60, no. 8, pp. 1500–1505. *https://doi.org/10.2320/ matertrans.MF201942*
7. Bubnov V.A., Korotovskikh V.K., Kostenko S.G. Effect of the degree of plastic deformation on hardness of austenitic steel. *Chemical and Petroleum Engineering.* 2022, vol. 57, no. 11-12, pp. 1038–1042. *https://doi.org/ 10.1007/s10556-022-01043-x*
8. Wang Y., Tomota Y., Harjo S., Gong W., Ohmuraa T. In-situ neutron diffraction during tension-compression cyclic deformation of a pearlite steel. *Materials Science and Engineering: A.* 2016, vol. 676, pp. 522–530. *https://doi.org/10.1016/j.msea.2016.08.122*
9. Pan R., Ren R., Chen C., Zhao X. Formation of nanocrystalline structure in pearlitic steels by dry sliding wear. *Materials Characterization*. 2017, vol. 132, pp. 397–404. *https://doi.org/10.1016/j.matchar.2017.05.031*
10. Steenbergen M. Rolling contact fatigue: Spalling versus transverse fracture of rails. *Wear*. 2017, vol. 380-381, pp. 96–105. *https://doi.org/10.1016/j.wear.2017.03.003*
11. Vinogradov A., Estrin Y. Analytical and numerical approaches to modelling severe plastic deformation// *Progress in Materials Science*. 2018, vol. 95, pp. 172–242. *https://doi.org/ 10.1016/j.pmatsci.2018.02.001*
12. Nikas D., Zhang X., Ahlström J. Evaluation of local strength via microstructural quantification in a pearlitic rail steel deformed by simultaneous compression and torsion. *Materials Science and Engineering: A.* 2018, vol. 737, pp. 341–347. *https://doi.org/10.1016/j.msea. 2018.09.067*
13. Skrypnyk R., Ekh M., Nielsen J.C.O., Pålsson B.A. Prediction of plastic deformation and wear in railway crossings – Comparing the performance of two rail steel grades. *Wear*. 2019, vol. 428–429, pp. 302–314. *https://doi.org/ 10.1016/j.wear.2019.03.019*
14. Rong K-j., Xiao Ye-l., Shen M-x., Zhao H-p., Wang W-J., Xiong G-Y. Influence of ambient humidity on the adhesion and damage behavior of wheel–rail interface under hot weather condition. *Wear*. 2021, vol. 486-487, article 204091. *https://doi.org/10.1016/j.wear. 2021.204091*
15. Li X.C., Ding H.H., Wang W.J., Guo J., Liu Q.Y., Zhou Z.R. Investigation on the relationship between microstructure and wear characteristic of rail materials. *Tribology International*. 2021, vol. 163, article 107152. *https://doi.org/10.1016/j.triboint.2021.107152*
16. Miranda R.S., Rezende A.B., Fonseca S.T., Sinatora A., Mei P.R. Fatigue and wear behavior of pearlitic and bainitic microstructures with the same chemical composition and hardness using twin-disc tests. *Wear*. 2022, vol. 494-495, article 204253. *https://doi.org/ 10.1016/j.wear.2022.204253*
17. Pereira H.B., Dias Alves L.H., Rezende A.B., Mei P.R., Goldenstein H. Influence of the microstructure on the rolling contact fatigue of rail steel: Spheroidized pearlite and fully pearlitic microstructure analysis. *Wear*. 2022, vol. 498-499, article 204299. *https://doi.org/10.1016/j.wear.2022.204299*
18. Pan R., Chen Yu., Lan H., Ren R. Investigation into the microstructure evolution and damage on rail at curved tracks. *Wear*. 2022, vol. 504-505, article 204420. *https://doi.org/ 10.1016/j.wear.2022.204420*

19. Zhang S-Yu., Spiryagin M., Lin Q., Ding H-h., Wu Q., Guo J., Liu Q-Yu., Wang W-J. Study on wear and rolling contact fatigue behaviours of defective rail under different slip ratio and contact stress conditions. *Tribology International*. 2022, vol. 169, article 107491. *https://doi.org/10.1016/j.triboint.2022.107491*

20. Ivanov Yu.F., Gromov V.E., Nikitina E.N. *Bainitic constructional steel. Structure and Hardening Mechanisms.* Cambridge, 2017, 121 p.

21. Yildirim C., Jessop C., Ahlström J., Detlefs C., Zhang Y. 3D mapping of orientation variation and local residual stress within individual grains of pearlitic steel using synchrotron dark field X-ray microscopy. *Scripta Materialia*. 2021, vol. 197, article 113783. *https://doi.org/10.1016/j.scriptamat.2021.113783*

22. Rybin V.V. *Large plastic deformations and destruction of metals.* Moscow: Metallurgy, 1986, 224 p.

23. Hirsch P., Hovey A., Nicholson P., Pasley D., Whelan M. *Electron microscopy of thin crystals*. United Kingdom: Butterworth/Heinemann, 1968, 574 p.

24. Carter C.B., Williams D.B. *Transmission Electron Microscopy.* Berlin: Springer International Publishing, 2016, 518 p.

25. Ivanov Yu.A., Gromov V.E., Yuriev A.A., Kormyshev V.E., Rubannikova Yu.A., Semin A.P. Deformation strengthening mechanisms of rails in extremely long-term operation. *Journal of Materials Research and Technology*. 2021, vol. 11, pp. 710–718. *https://doi.org/10.1016/j.jmrt.2020.12.107*

26. Yuriev A.A., Ivanov Yu.F., Gromov V.E., Rubannikova Yu.A., Starostenkov M.D., Tabakov P.Y. *Structure and properties of lengthy rails after extreme long-term operation.* Millersville: PA, USA: Materials Research Forum LLC, 2021, 194 p. *https://doi.org/10.21741/9781644901472*

27. Ivanov Yu.F., Yuriev A.A., Chen X., Kosterev V.B., Gromov V.E. Physical nature of strengthening mechanisms during extremely long-term operation of rails. *Izvestiya of Altai State University*. 2021, vol. 117, no. 1, pp. 33–39. *https://doi.org/10.14258/izvasu(2021)1-05*

28. Ivanov Yu.F., Glezer A.M., Kuznetsov R.V., Gromov V.E., Shliarova Yu.A., Semin A.P., Sundeev R.V. Fine structure formation in rails under ultra long-term operation. *Materials Letters*. 2022, vol. 309, no.4, article 131378. *http://dx.doi.org/10.1016/j.matlet.2021.131378*

29. Ivanov Yu.F., Gromov V.E., Aksenova K.V., Kuznetsov R.V., Kormyshev V.E., Vashchuk E.S. Evolution of the structure of rail steel during compression. *Russian Metallurgy (Metally)*. 2022, vol. 10, pp. 1192–1197. *https://https://doi.org/10.1134/S0036029522100354*

30. Aksenova K.V., Gromov V.E., Ivanov Yu.F., Vashchuk E.S., Peregudov O.A. Evolution of the structure of lamellar pearlite of rail steel under compression deformation. *Izvestiya. Ferrous Metallurgy*. 2022, vol. 65, no. 9, pp. 654–661. (In Russ.). *https://doi.org/10.17073/0368-0797-2022-9-654-661*

31. Saltykov S.A. *Stereometric metallography*. Moscow: Metallurgy, 1970, 376 p.

32. Chernyavskii K.S. *Stereology in metal science*. Moscow: Metallurgy, 1977, 280 p.

33. Goldstein M.I. Farber, B.M. *Dispersion hardening of stell*. Moscow: Metallurgy, 1979, 208 p.

34. Yao M.J., Welsch E., Ponge D., Haghighat S.M.H., Sandlöbes S., Choi P., Herbig M., Bleskov I., Hickel T., Lipinska-Chwalek M., Shantraj P., Scheu C., Zaefferer S., Gault B., Raabe D. Strengthening and strain hardening mechanisms in a precipitation-hardened high-Mn lightweight steel. *Acta Materia*. 2017, vol. 140, pp. 258–273. *https://doi.org/10.1016/j.actamat.2017.08.049*

Сведения об авторах

Юрий Федорович Иванов, *д.ф.-м.н., профессор, главный научный сотрудник*, Институт сильноточной электроники СО РАН
E-mail: yufi55@mail.ru
ORCID: 0000-0001-8022-7958

Михаил Анатольевич Порфирьев, *соискатель кафедры естественнонаучных дисциплин им. проф. В.М. Финкеля,* Сибирский государственный индустриальный университет
E-mail: mporf372@gmail.com
ORCID: 0000-0003-3602-5739

Виктор Евгеньевич Громов, *д.ф.-м.н., профессор, заведующий кафедрой естественнонаучных дисциплин им. профессора В.М. Финкеля,* Сибирский государственный индустриальный университет
E-mail: gromov@physics.sibsiu.ru
ORCID: 0000-0002-5147-5343

Наталья Анатольевна Попова, *к.т.н., старший научный сотрудник кафедры физики,* Томский государственный архитектурно-строительный университет
E-mail: popova-44@mail.ru
ORCID: 0000-0001-8823-4562

Юрий Сергеевич Серенков, *д. культурологии, доцент, заведующий кафедрой филологии,* Сибирский государственный индустриальный университет
E-mail: juriyy-serenkov@rambler.ru

Аршад Нур Сиддики, *д.ф.н., профессор,* Джамия Миллия Исламия

E-mail: ansiddiqui@jmi.ac.in
ORCID: 0000-0002-3573-8385

Виталий Владиславович Шляров, *аспирант кафедры естественнонаучных дисциплин им. профессора В.М. Финкеля, научный сотрудник лаборатории электронной микроскопии и обработки изображений,* Сибирский государственный индустриальный университет
E-mail: shlyarov@mail.ru
ORCID: 0000-0001-8130-648X

Information about the authors

Yurii F. Ivanov, *Dr. Sci. (Phys.-Math.), Prof., Chief Researcher of the Laboratory of Plasma Emission Electronics*, Institute of High-Current Electronics
***E-mail*:** yufi55@mail.ru
ORCID: 0000-0001-8022-7958

Mikhail A. Porfir'ev, *Applicant of the Department of Natural Sciences named after. prof. V.M. Finkel,* Siberian State Industrial University
E-mail: mporf372@gmail.com
ORCID: 0000-0003-3602-5739

Viktor E. Gromov*, Dr. Sci. (Phys.-Math.), Prof., Head of the Chair of Science named after V.M. Finkel',* Siberian State Industrial University
***E-mail*:** gromov@physics.sibsiu.ru
ORCID: 0000-0002-5147-5343

Natal'ya A. Popova, *Cand. Sci. (Eng.), Senior Researcher of the Chair of Physics,* Tomsk State University of Architecture and Building
E-mail: popova-44@mail.ru
ORCID: 0000-0001-8823-4562

Yurii S. Serenkov, *Dr. Sci. (Culture Studies), Assistant Prof., Head of the Chair of of Philology,* Siberian State Industrial University
E-mail: juriyy-serenkov@rambler.ru

Arshad Nur Siddiquee*, D.Sci. (Philosophy), Professor,* Jamia Millia Islamia
E-mail: ansiddiqui@jmi.ac.in
ORCID: 0000-0002-3573-8385

Vitalii V. Shlyarov, *Postgraduate of the Chair of Science named after V.M. Finkel', Researcher, Laboratory of Electron Microscopy and Image Processing,* Siberian State Industrial University
E-mail: shlyarov@mail.ru
ORCID: 0000-0001-8130-648X

Авторы заявляют об отсутствии конфликта интересов.
The authors declare that there is no conflict of interest.

Поступила в редакцию 15.08.2023
После доработки 28.08.2023
Принята к публикации 31.08.2023

Received 15.08.2023
Revised 28.08.2023
Accepted 31.08.2023